University of Washington
Department of Civil and Environmental Engineering

HYDRAULIC MODELING STUDY: SIMULATED JUVENILE SALMON MIGRATION PAST COOLING-WATER DISCHARGE JET

R. E. Nece
J. C. Kent

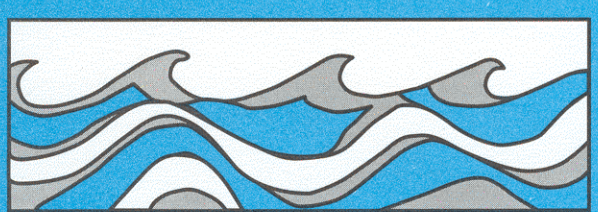

Water Resources Series
Technical Report No. 31
July 1971

Seattle, Washington
98195

Department of Civil Engineering
University of Washington
Seattle, Washington 98195

HYDRAULIC MODELING STUDY: SIMULATED JUVENILE SALMON MIGRATION PAST COOLING-WATER DISCHARGE JET

R. E. Nece
J. C. Kent

Water Resources Series
Technical Report No. 31

July 1971

Charles W. Harris Hydraulics Laboratory

Department of Civil Engineering

University of Washington
Seattle, Washington 98105

HYDRAULIC MODEL STUDY:

SIMULATED JUVENILE SALMON MIGRATION

PAST COOLING-WATER DISCHARGE JET

by

Ronald E. Nece and Joseph C. Kent

July 1971

Technical Report No. 31

Prepared for
Pacific Northwest Laboratory, Battelle Northwest Institute
Richland, Washington

TABLE OF CONTENTS

ACKNOWLEDGMENT

The study reported here was performed for the Pacific Northwest Laboratory of the Battelle Northwest Institute, Richland, Washington, under the terms of Special Agreement BSA-692, March 18, 1971. Mr. R. D. Harr served as the sponsor's agent during the study.

The work was conducted at the C. W. Harris Hydraulics Laboratory, University of Washington, by Joseph C. Kent, Associate Professor of Civil Engineering (Principal Investigator) and Ronald E. Nece, Professor of Civil Engineering.

LIST OF FIGURES

I. INTRODUCTION

The objectives of the model study reported here were to determine if the hydraulic characteristics of a cooling water discharge jet allow downstream migrating juvenile salmon to enter the relatively undiluted portion of the jet and, if the salmon do enter the jet, to determine where they enter the jet and to estimate their temperature exposure.

The study was made on an idealized cooling water discharge. Initial specifications of the discharge to be studied are listed below; the notation is defined in Fig. 1.

(a) Jet discharge normal to river flow.

(b) Jet discharge at river bottom.

(c) Jet discharge at river center.

(d) Jet discharge (T_0) 13 degrees centigrade above ambient river water temperature (T_R).

(e) Pipe diameter d = 10 feet.

(f) Effluent velocity U_0 = 9.8 feet per second.

(g) River velocity V = 4.0 feet per second.

(h) River depth D = 20 feet.

All tests perfonned were made at the 13° temperature differential and at the single prescribed set of velocities U_0 and V. Results are reported for river depths D of 20 feet and 40 feet. In the absence of design details for the outfall the simple schematic configuration shown in Fig. 1 was adopted, and tests were conducted with equivalent prototype outfall lengths L of 0, 38, and 76 feet in order to investigate effects of length changes in outfall pipes upon flow conditions near the discharge port. The schematic 'river' section had a horizontal bottom and vertical

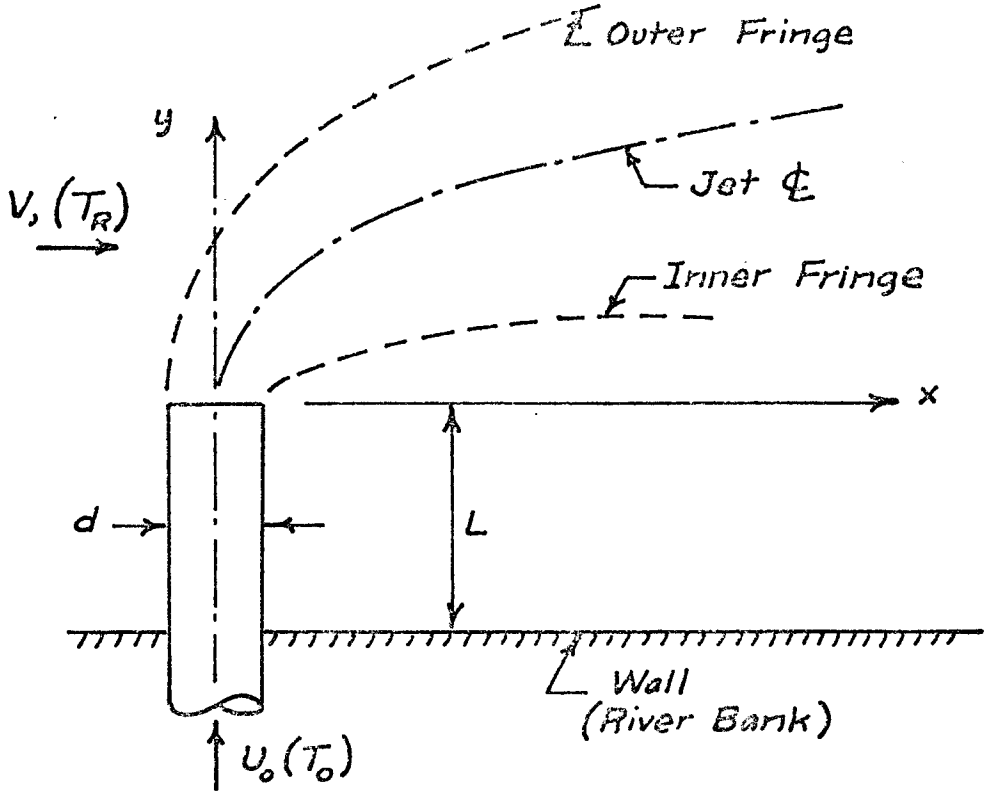

Plan View

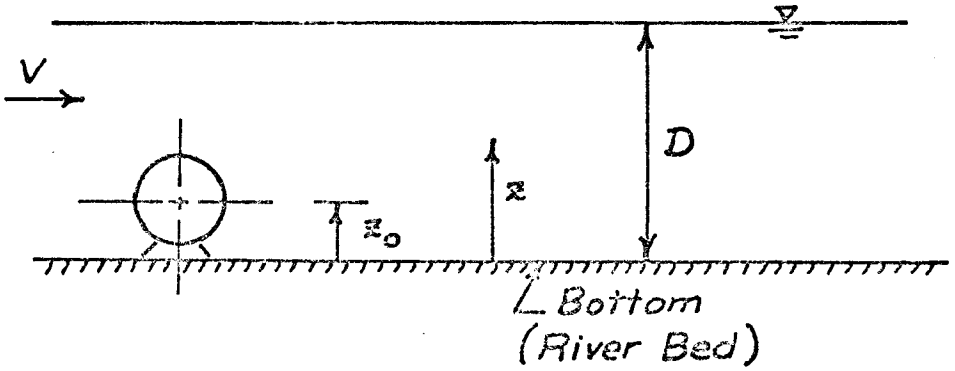

Elevation View

Figure 1. Definition and Notation Sketch

banks; the equivalent channel width was 320 feet.

The model was to incorporate the following:

(a) Dyed effluent.

(b) Heated effluent.

(c) Neutral-buoyant bubbles to simulate downstream migrating fish.

(d) Adjustable position of bubble injection points.

(e) Vertical and horizontal photography of the bubble flows (paths of simulated fish) to show entrainment of bubbles as a function of position of the bubble injection system.

The study as conducted complied with items a-d. A visual observation scheme was adopted for the fish tracking runs; reasons for this procedural change are given in Chapter II. Jet trajectory and profile observations were made, and limited data obtained on the temperature field within the diffusing jet.

Most of the experimental data are presented in graphical form. Data on fish passage past the discharge jet are given in semi-qualitative form as dictated by the statistical nature of variations in paths taken by individual neutrally buoyant bubbles through the turbulent flow field.

II. MODEL DESIGN AND OPERATION

A. Scale Selection

The schematic model was built to an undistorted scale ration of 1:80. The scale selected was compatible with water supply capabilities in the laboratory, in particular the available hot water source. Froude law scaling was applicable for the free-surface model; all conduit dimensions and water velocities were sufficiently high so that all flows were turbulent and Reynolds number effects could be ignored.

The model was 'schematic' in that there was no attempt to model a river width; however, as the prototype discharges in the middle of a wide river, the only width requirement in the laboratory test was that the width of model channel be sufficiently wide so as not to have the far bank interfere with the discharge jet.

The flow field of concern to this study was in the near vicinity of the discharge end of the outfall. Ackers (1969) has presented the rationale for selecting an undistorted physical model for studying the "near field" of buoyant jets. The pertinent similarity criterion then becomes the densimetric Froude number F of the cooling water jet,

$$F = \frac{U_0}{\sqrt{g \frac{\Delta\rho}{\rho_0} d}}$$

where ρ_0 = density of the fluid in discharge stream

$\Delta\rho = \rho_{river} - \rho_0$

g = gravitational acceleration.

The non-linear relationship between water temperature and density requires that density differentials be reproduced for strict densimetric Froude law similarity. In the absence of specific prototype values of T_R, it was decided to operate the laboratory model at $\Delta T = 13°C$. For a probable range of prototype T_R values of 7.2°C to 15.5°C (45°F - 60°F) the corresponding values of F are 13.5 and 10.4, respectively. Fan and Brooks (1966) and Anwar (1969) have shown that over this F range for buoyant jets discharging into an infinite stagnant receiving fluid there is very little effect on jet trajectory within the relatively small z/d and x/d distances of concern in the present test. Therefore, the simplicity of using the constant $\Delta T = T_0 - T_R = 13°C$ in the laboratory was justified.

Similarity of the other pertinent flow parameter, the ratio U_0/V, was insured by setting the appropriate discharges in the undistorted model.

B. Description

The model was provided with two separate flow systems, for the river channel and for the outfall.

River flow was supplied from the laboratory recirculatory system. Water was delivered to the model from a constant head tank through a 6-inch pipe containing a flow meter (Dall tube) which measured river discharges. The supply pipe discharged into a baffled head box attached to the flow channel through a faired transition. The test channel was 12 feet long, 4 feet wide, with a horizontal wood bottom painted white for visibility purposes and transparent plastic sidewalls 10 inches high. Flow rates were controlled by a valve on the supply pipe to the head box; river depths were controlled with an adjustable weir at the downstream

end of the channel. The channel is shown in Fig. 2.

The cooling water was supplied from a separate recirculatory system incorporating a pump, storage reservoir, and constant head tank. Hot water was obtained from a hose connection to the laboratory domestic hot water supply; model flow requirements exceeded the constant hot water flow available, so test durations were limited to the amount of heated water stored prior to each run in the 17 cubic foot (effective volume) partially insulated reservoir. Cooling water discharges were measured with a calibrated $^{5}/_{8}$-inch throat venturi meter in the outfall supply line. Reservoir temperatures were monitored by a sealed immersible thermometer with a dial gage.

The outfall conduit was formed by a 1.5-inch I.D. plastic tube inserted through a sleeve in one side wall. The outfall was located 3 feet (240 feet, prototype) downstream from the channel entrance; the outfall centerline elevation above channel bottom was z_0 = 6.67 feet, prototype. The inserted length L of the outfall was adjustable; in Fig. 2, the outfall is shown in the L = 0 position.

C. Determination of Jet Characteristics

Flows in all runs were set to match prototypes values, following the Froude scaling law: (velocity ratio) proportional to (length ratio)$^{\frac{1}{2}}$.

Velocity	Prototype	Model
U_0	9.8 fps	9.8 ÷ $(80)^{\frac{1}{2}}$ = 1.095 fps
V	4.0 fps	4.0 ÷ $(80)^{\frac{1}{2}}$ = 0.446 fps.

Jet configurations were determined through visual observations of the cooling water discharge, dyed for these runs with potassium permanganate. Transparent coordinate grids ruled with 10-foot (prototype) spacings were positioned above the channel (resting on the sidewalls) and on the

Figure 2. Test Channel

sidewall through which passed the outfall. All sightings were taken by eye, with a combination square used to eliminate parallax error. The outer fringes of the jet as observed from above, the approximate centerline as seen in plan view, and the visual estimate of the surface disturbance ('boil') where the jet intersected the river surface were traced on the horizontal grid above the channel and then transferred to tracing paper. The upper fringe of the jet as viewed through the sidewall also was traced in the same way.

Although not a part of the original test specifications, it was considered appropriate to determine some of the temperature field in the jet. Readings were taken by hand-held thermometer, positioned by use of the two orthogonal grids systems. A limited number of readings were taken; vertical temperature profiles of three readings were taken at a few stations on the jet centerline as determined from the plan view trajectory tracing, along the jet fringes close to the outfall exit, and in the boil area. Temperatures of the river flow and of cooling water discharge inside the outfall were read routinely.

D. Simulation of Fish Paths

Downstream migrant salmon were simulated by red-dyed, neutrally bouyant, immiscible drops formed from a mixture of xylene and dibutyl phthalate. Drops were released into the river flow at injection points upstream from the outfall by use of a syringe fitted with a number 19 hypodermic needle. The needle was oriented vertically with its tip at the desired elevation below the river surface; only a slight pressure on the plunger was required to release individual bubbles having zero initial vertical velocity. The x-y-z coordinates of the injection points are

given in Chapter III. Bubble sizes ranged from 1 to 3 mm. Injection depths were limited to 10 feet for the D = 20 feet runs and to 15 feet for D = 40 because downstream migrant salmon most commonly drift in the upper layers of the stream.

Visual procedures were used for the fish passage tests in place of the initially specified photographic methods. A number of reasons can be cited. A major reason was the question of the statistical (time-varying) nature of the bubble paths, due to flow turbulence. Turbulence was greater for the D = 40 feet runs; with V held constant the flow rate through the head box was doubled, increasing turbulent eddy production that was not fully removed by the baffles. Consequently, there was more consistency in bubble paths for the more important D = 20 feet case. Although no consideration was given to scaling turbulence, it is thought that the model flow for D = 20 is more representative of prototype river flows. Even for the 20-foot depth it was observed (predictably) that not all bubbles injected at the same point moved along identical paths; as a consequence, instantaneous or even streak photographs showing even a large number of bubbles might not show either the statistically most common path or the variation of path scatter which occurs over time. A counting procedure was used. Depending on the pathline scatter, either dye drop counts were made over a time period within various 10-foot spacings of y-coordinates at various x-stations (downstream from the injection point) or in the case of greater path consistency the y-coordinate of the "concentration" path of bubbles passing the given x-station was determined, along with the approximate band width (in y-coordinates) within which all bubbles passed. Observations of bubble paths in the vertical plane, made through the sidewall, were more qualitative.

Water clarity was another problem which dictated not using photographic methods, as horizontal sight distances through the water were limited to 1-1.5 feet (model) for most runs, a situation which would have made horizontal photography difficult. Also, of course, in final analysis, the visual counting procedure was faster and cheaper; this budgetary consideration was important. On balance, the procedures followed are considered to give results equal to, if not better than, photographic data which might have been obtained within the limits of the study.

III. RESULTS

A. Jet Characteristics

Jet profile data are shown in Fig. 3 for D = 20 feet and in Fig. 4 for D = 40 feet, for values of L = 0, 38, and 76 feet. Only the jet centerline is shown in the plan view; jet fringe locations can be estimated on the plots by faired lines connecting the 5-foot radius point at the conduit outlet to the extremity of the boil region. The profile data on Figs. 3 and 4 are 'time-averaged'; as with all turbulent jets, those investigated here did not remain stationary with time but continuously underwent lateral shifting about the mean centerline location shown.

The data show there is little effect of either D or L on centerline trajectories for that portion of the jet close to the outfall - say, to $x = \pm$ 40 feet, which includes the area where the jets have just intersected the river surface for the D = 20 case. The same comment applies to the behavior of the upper edge of the jet as seen in elevation view. The tests indicate that the outfall conduit configuration (i.e., length L extending into the stream from a bank) has little effect on the jet shape. There was no apparent effect from the opposite bank on jet locations.

A check run was made with zero temperature (hence density) differential between river and outfall flows. Results of the $\Delta T = 0$ run are almost identical close to the outlet port with those of the $\Delta T = 13°C$ runs, while further downstream the delayed appearance of the boil at the free surface shows the non-buoyancy effects. These results confirm that essentially the same jet configuration exists close to the outlet (where temperatures of concern to fish passage are highest) over a wide range of densimetric Froude numbers, and hence for a model study the strict equality of F values

discussed in Chapter I need not be obtained.

By implication, as neither the outfall geometry, as characterized by L/D, nor $\mathbb{F}$ have significant effects on jet forms close to the outlet, the controlling variable is the ratio U_0/V which was held constant. Shown on Figs. 3 and 4 is a trajectory predicted by an empirical expression for round jet profiles in a relatively unconfined cross-flow as proposed by Callahan and Ruggeri (1948). For zero density differential, this relationship in terms of the present variables is

$$\left(\frac{Y}{D}\right)^{1.65} = 2.91 \left(\frac{U_0}{V}\right)\left(\frac{x}{D}\right)^{0.50}$$

This equation is selected as a representative one available in the literature. Also shown in Figs. 3 and 4 is one point, obtained by extrapolating results of Fan (1967) for $\mathbb{F}$ = 10 to U_0/V = 2.45 of the present test. For both of these other references, however, the initial jet velocity was in the direction of the gravitational (buoyancy) force, not normal to it as in the present study. The jets observed here show a much faster deflection from their initial direction because the confinement of the relatively small D/d eliminates an 'escape route' for the river water to move around the entering jet; conservation of momentum in the x-direction dictates the rapid jet deflection.

The 40-foot river depth run does not simulate prototype conditions. For strict modeling purposes, it would have been more appropriate to make V = 5.66 fps (prototype) in accordance with the open channel relationship $V \propto D^{0.5}$ for wide open channels. For the increased V, the cooling water jet would be deflected more quickly than was the case in the present tests;

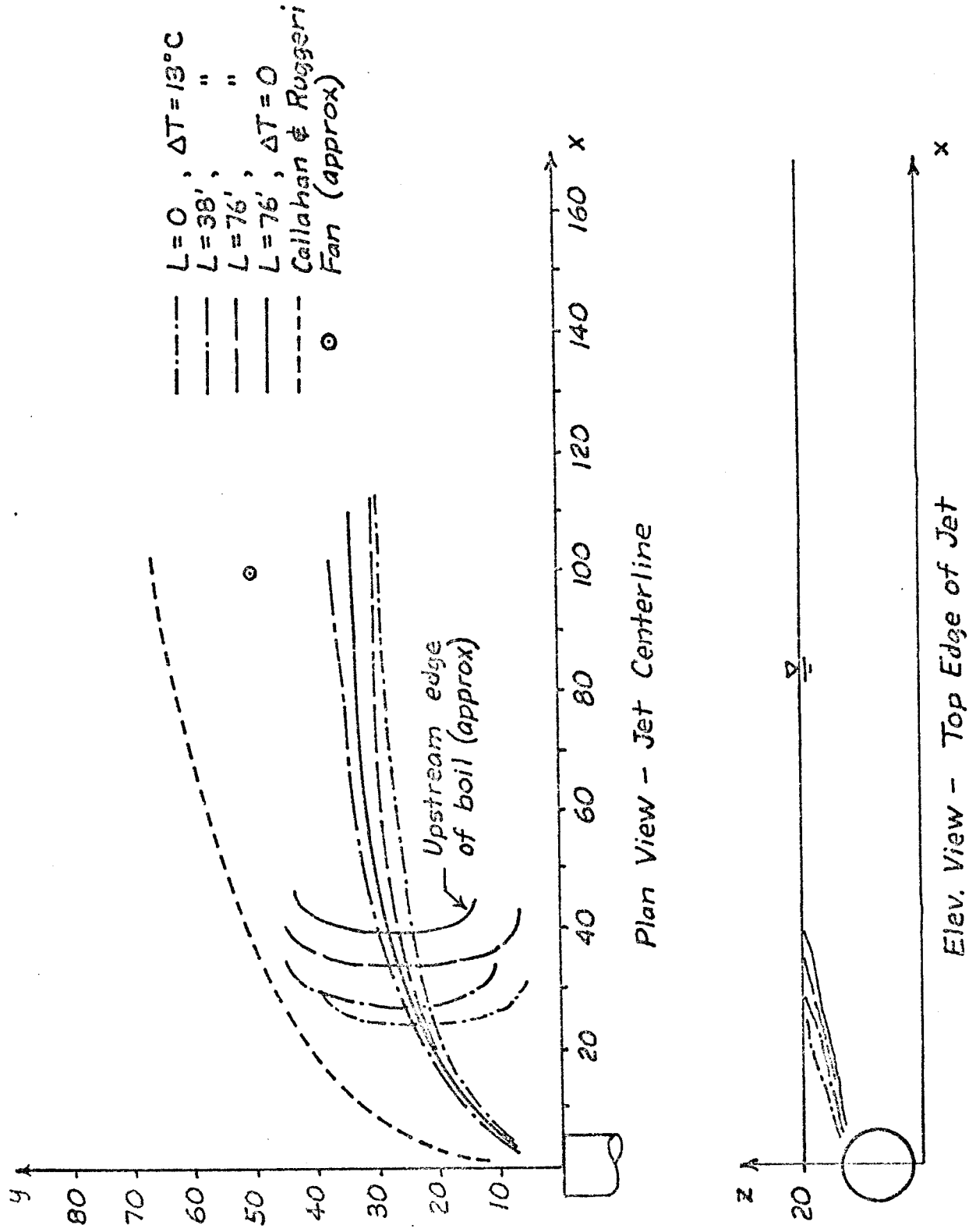

Fig. 3 Jet Trajectories, D = 20 feet

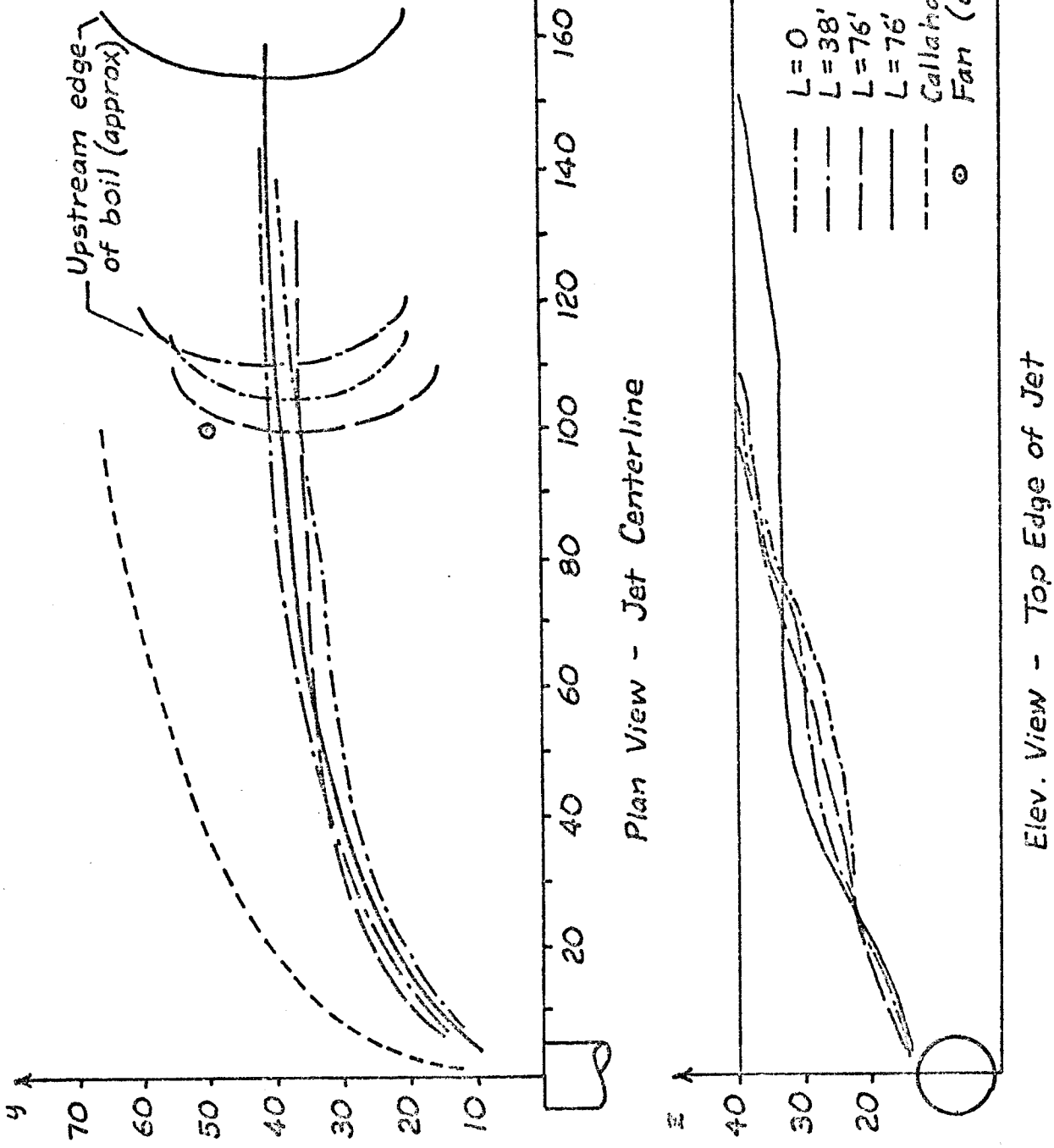

Figure 4. Jet Trajectories, D = 20 Feet

further extrapolating the laboratory results of Fan (1967), jet centerline y-coordinates would be reduced by about one-third.

Temperature data and jet edge locations are given for D = 20 at L = 76 and 0, and for D = 40 at L = 76 and 0, in Figs. 5 through 8, respectively. These are the four cases for which fish passage data were obtained, and span the range of test variables. The temperature readings are repeated in Figs. 9-12, discussed in Section B. Actual temperature differentials between cooling water and river flow varied over the range 11.5°-14.9°C during the various model tests; temperature values ΔT shown on the plots are all adjusted to an initial 13°C differential. The ΔT value given is defined as $\Delta T = T - T_R$, where T is the local temperature at the point.

The limited temperature data indicate that jet temperatures decrease more rapidly with axial distance from the outlet than predicted if temperature is used as the 'concentration' in the analyses of Fan and Brooks (1966) and Anwar (1969) for buoyant jets in stagnant ambient fluids. Also, temperatures tend to remain higher at the greater depths because vertical jet diffusion is restricted by the river bottom.

For the runs with river depth D = 40 feet, temperature measurements were restricted to z distances of 0, 10, and 20 feet because only farther downstream, under the boil, do temperature rises ΔT at z = 20 feet reach a value of more than 2°C. Data for the D = 20 feet runs, where readings were taken at the z = 0, 5, 10, and 15-foot levels, indicate that temperatures ΔT near the water surface can reach 3°C downstream from the boil. The temperature fields were not sampled comprehensively, and the 'centerline' readings may not be maxima. Due to the turbulent fluctuations in the jet local temperatures likewise underwent large fluctuations, especially at the

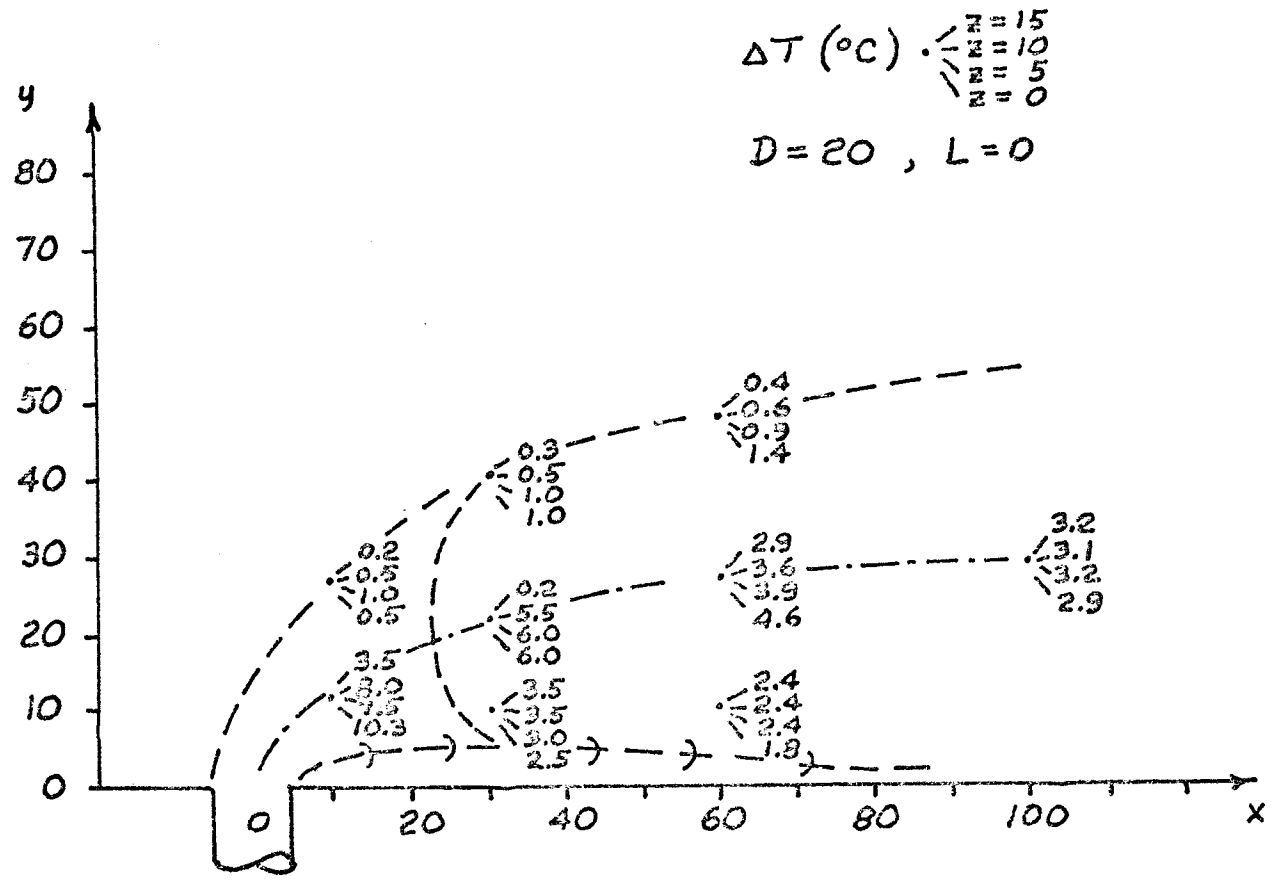

Figure 6. Jet Boundaries and Temperatures,

D = 20 Feet, L = 0

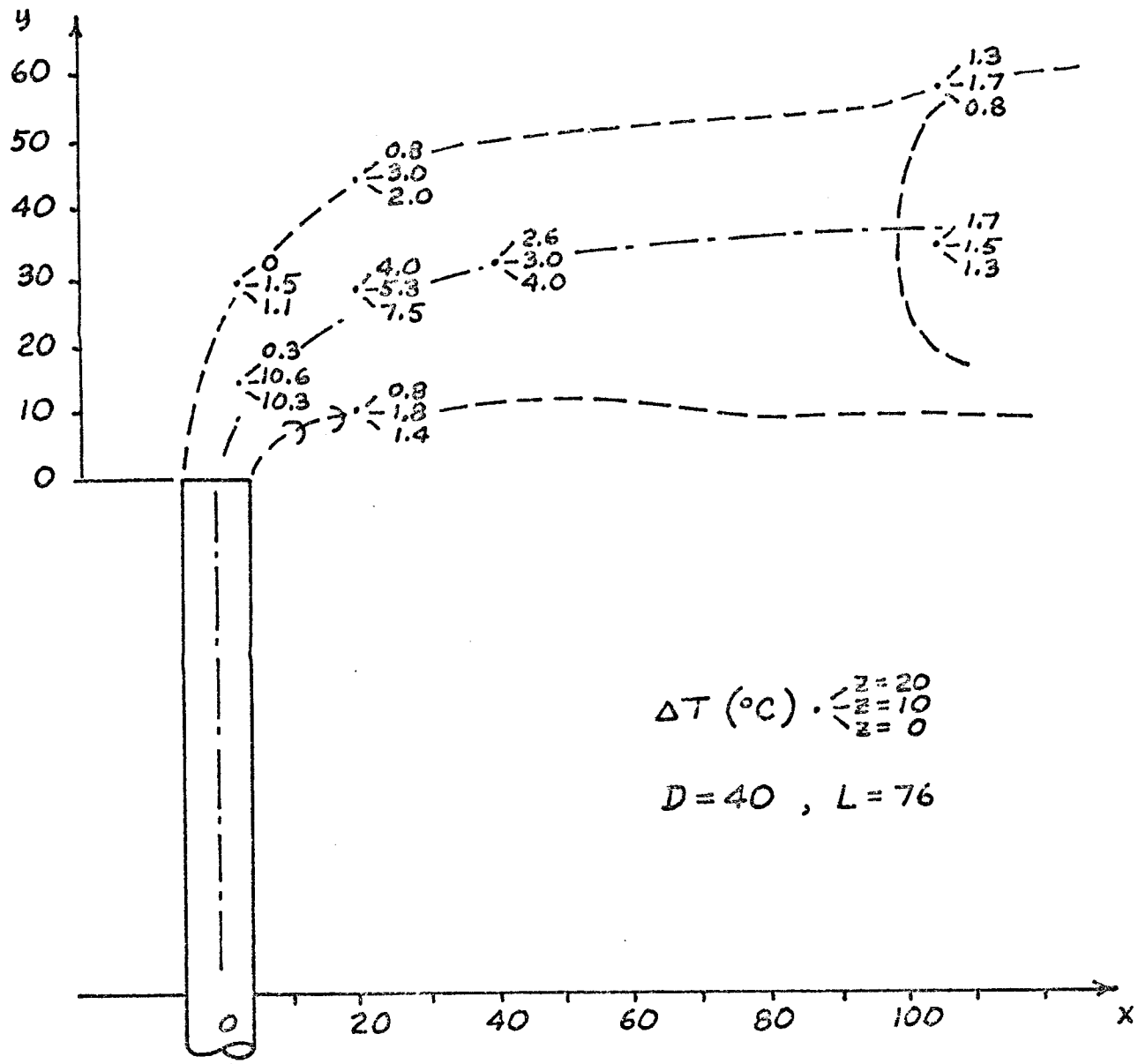

Figure 7. Jet Boundaries and Temperatures,

D = 40 Feet, L = 76 Feet

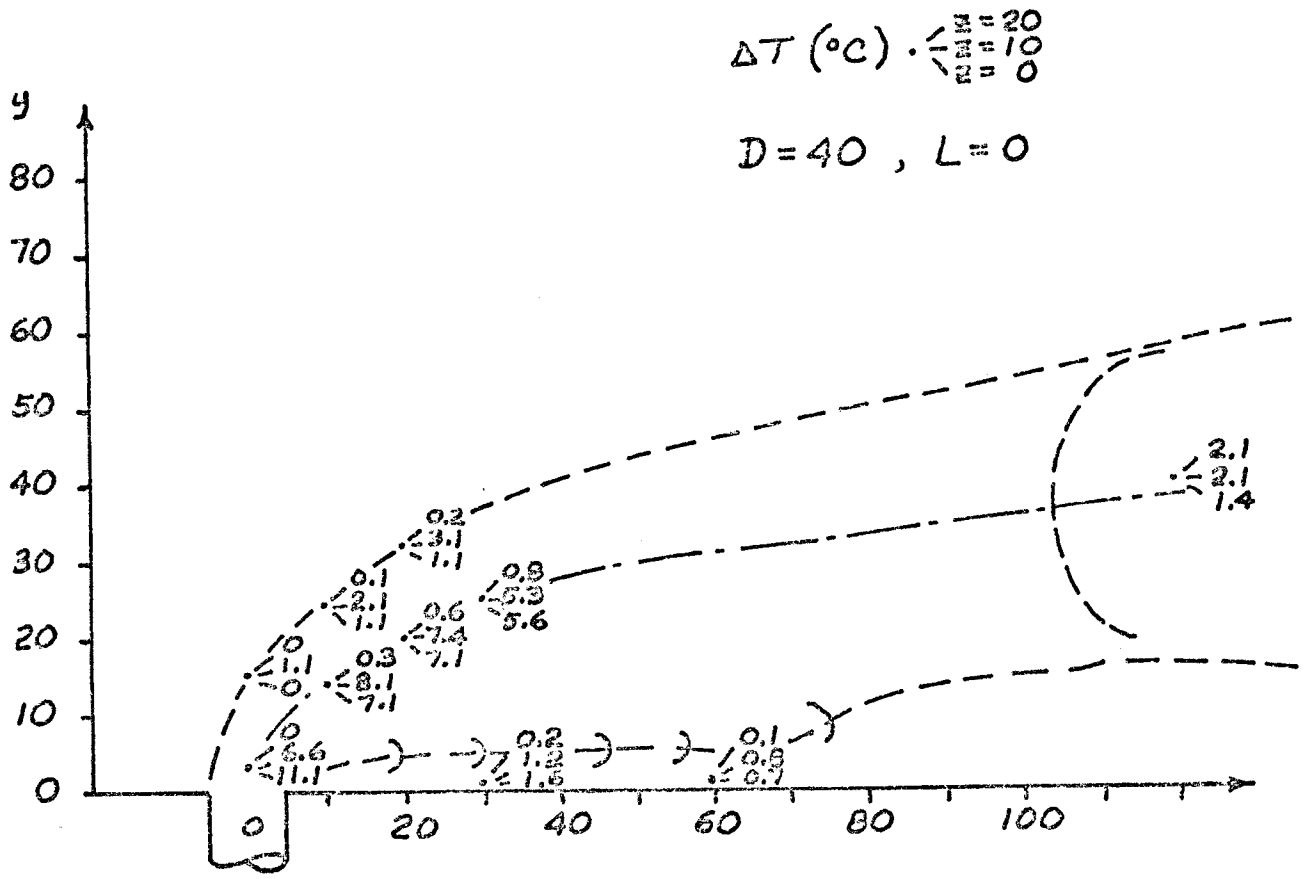

Figure 8. Jet Boundaries and Temperatures,

D = 40 Feet, L = 0

jet boundaries where ΔT values given are averages of ΔT's having total excursions of 1°C or more in many cases.

The small arcs drawn across the inner fringe lines on Figs. 5-8 indicate the presence of back eddies which were not present in any significant degree along the outer fringes. In the upper flow levels the eddies were more pronounced for the 20-foot river depth. For L = 76, the strongest eddy was located just downstream from the conduit and was a result of the displacement effect of the conduit itself on the river flow. For L = 0, the strongest eddy was a clockwise (plan view) back eddy just downstream from the boil; the comparable eddy for L = 76 feet was much weaker, as the river flow around the diffusing jet was much less confined. The effects of these eddies on fish passage are discussed in the following section.

B. Fish Pathlines past Cooling-Water Jet

1. D = 20 feet

Simulated fish pathlines for the 20-foot depth are shown in Figs. 9-12. Each figure shows plan views of the paths for one L-injection level z combination.

Dye drops were injected for all cases at the station x = -100 feet, where the flow is nearly uniform. Injections were limited to depths of 5 and 10 feet below the surface (z = 15 and 10 feet, respectively) at various stations y. Observations were made at x = 0 (where the bubbles crossed the conduit centerline) for both outfall lengths and at x = 30 feet for L = 0 and at x = 40 feet for L = 76, these latter distances being approximately at the longitudinal centerline of the boil. On each figure the solid line represents the mean ('concentration') path of the bubbles, and dashed lines on either side of it represent extremes of the paths as viewed

from above; at the appropriate x-stations, numbers indicate the percentage of the dye drops injected at the corresponding y-station passing x within the band-width shown. Where the percentage is less than 100, the approximate value shown is based on bubble counts. Specific comments are given below for each outfall length.

L = 76 feet (Figs. 9-10): All 'fish' injected at either z = 15 or z = 10, at y = 20, were deflected outward past the jet and boil. For injection at y = 0, for each injection level about 5 percent of the drops were caught in the boil and another 5 percent surfaced in the boil. For injection at y = -20, at both levels the mean pathline passed over the end of the outfall; for z = 15, 5 percent were caught in the back eddy behind the boil and then moved into the boil, while for z = 10, 50 percent of the dye drops were caught in the boil and moved into areas of higher ΔT near the boil center. For the y = -40 injection point, 25 percent of the drops for z = 15 were caught in the eddy on the downstream side of the pipe, with this figure being 30 percent for the z = 10 level. In each case, 10 percent of the injected drops went into the boil before going into the main jet downstream.

All bubbles that moved within the band-widths rose vertically to pass over the conduit or jet near the outfall and then tended to drop back to a lower z-level downstream from the conduit. Travel times for these drops are about the same as for the undisturbed river flow.

No 'fish' entered the hottest part of the jet. Of the four paths shown, the most dangerous is that for injection point (y = -20, z = 10), where the most fish are drawn into the boil where ΔT exceeds 3°C at the lower levels. As a check, for an injection point of y = -15, z = 15, 25 percent of the drops were caught in the boil and 10 percent surfaced in the boil.

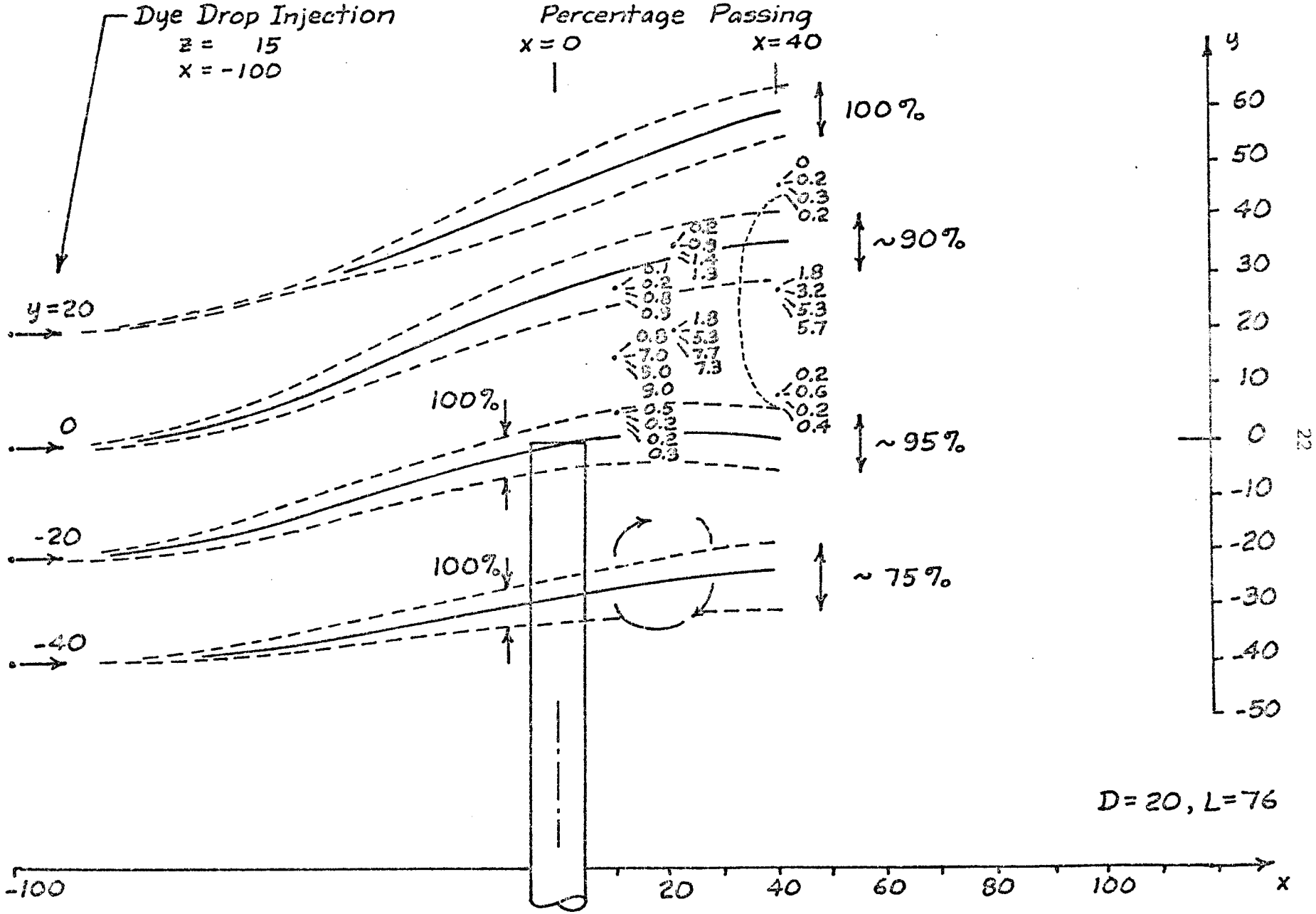

Figure 9. Fish Pathlines: D = 20 Feet, L = 76 Feet, z = 15 Feet

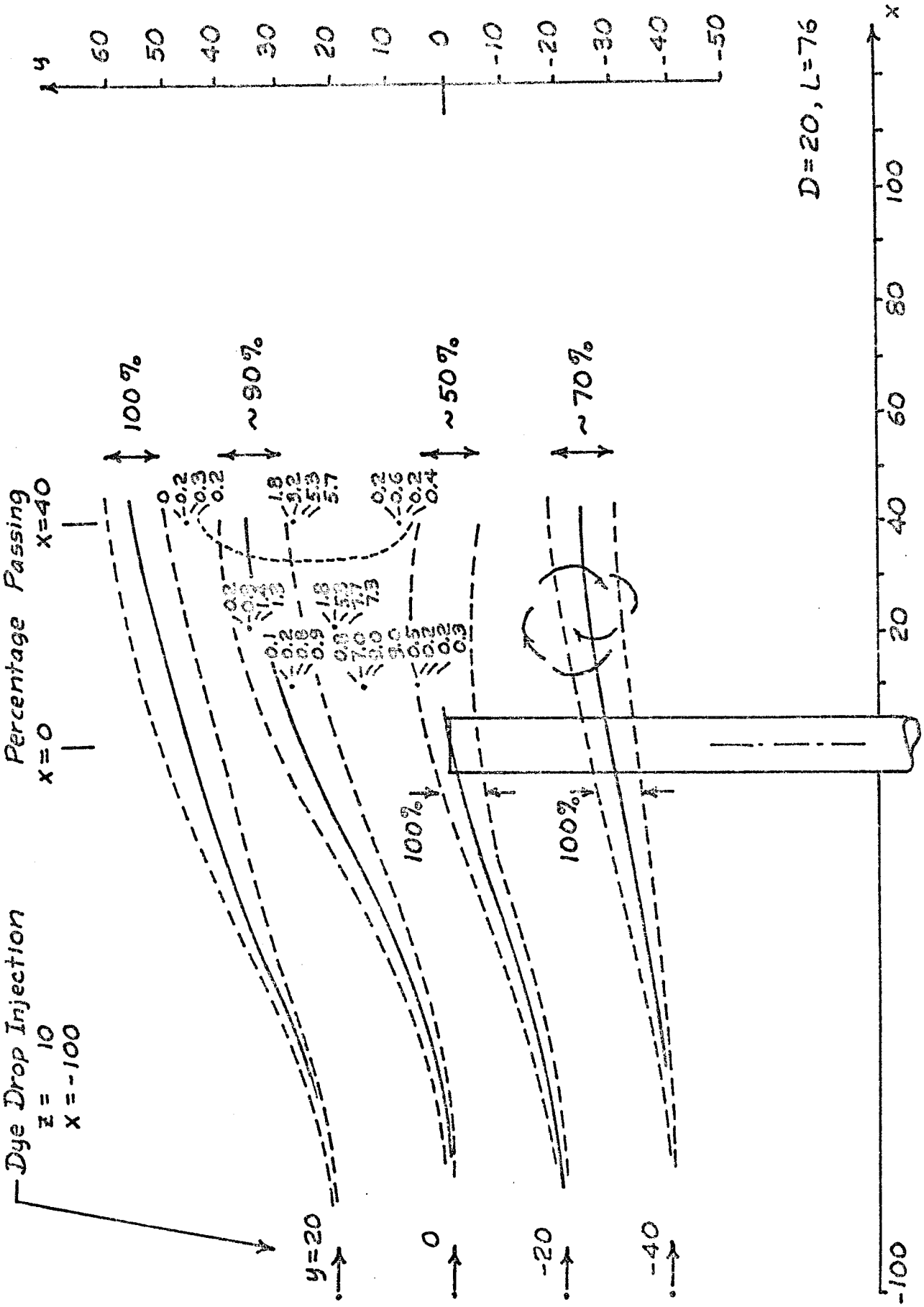

Figure 10. Fish Pathlines: D = 20 Feet, L = 76 Feet, z = 10 Feet

The worst fish approached in the upper 10 feet of water would appear to be at $z = 10$, passing through $x = -100$, $y = -15$. Although some travel times were measured for individual bubbles which were caught in boil or back eddy, these times were too erratic to be reported.

All fish approaching in the uniform upstream flow at $y \geq 20$ and at $y \leq -50$ seem to pass both the initial jet and boil without delay; 80 percent of the fish passing between these y-bounds also are not delayed, and those which do go into the boil area encounter maximum temperature rises ΔT of about 5°C. All fish approaching from upstream in the approximate zone $+20 > y > -30$ ultimately enter the jet far downstream where ΔT values are low.

Bubbles at depths greater than 10 feet may have greater percentages trapped in the boil, but none would move into the hottest part of the jet (from observed paths of bubbles which pass close to the outfall exit and were deflected upward following streamlines curving past the initial, hottest, part of the jet). As noted earlier, the 10-foot depth was considered a limiting depth for migrating salmon.

L = 0 (Figs. 11-12): All fish approaching at $y \geq 30$ would pass outside the boil formed with this limiting geometry configuration. Effects of the strong back eddy just downstream from the boil are pronounced. Dye drops caught in this eddy are shown as either drawn into the boil or drawn toward the wall. There were no defined 'paths' or even 'band-widths' that could be specified at $x = 30$ for those bubbles injected at $y = 10$ and at $y = 20$.

Motions of the bubbles in the vertical plane were comparable to those for the L = 76 feet tests. For injection levels $z = 15$ and 10, bubbles

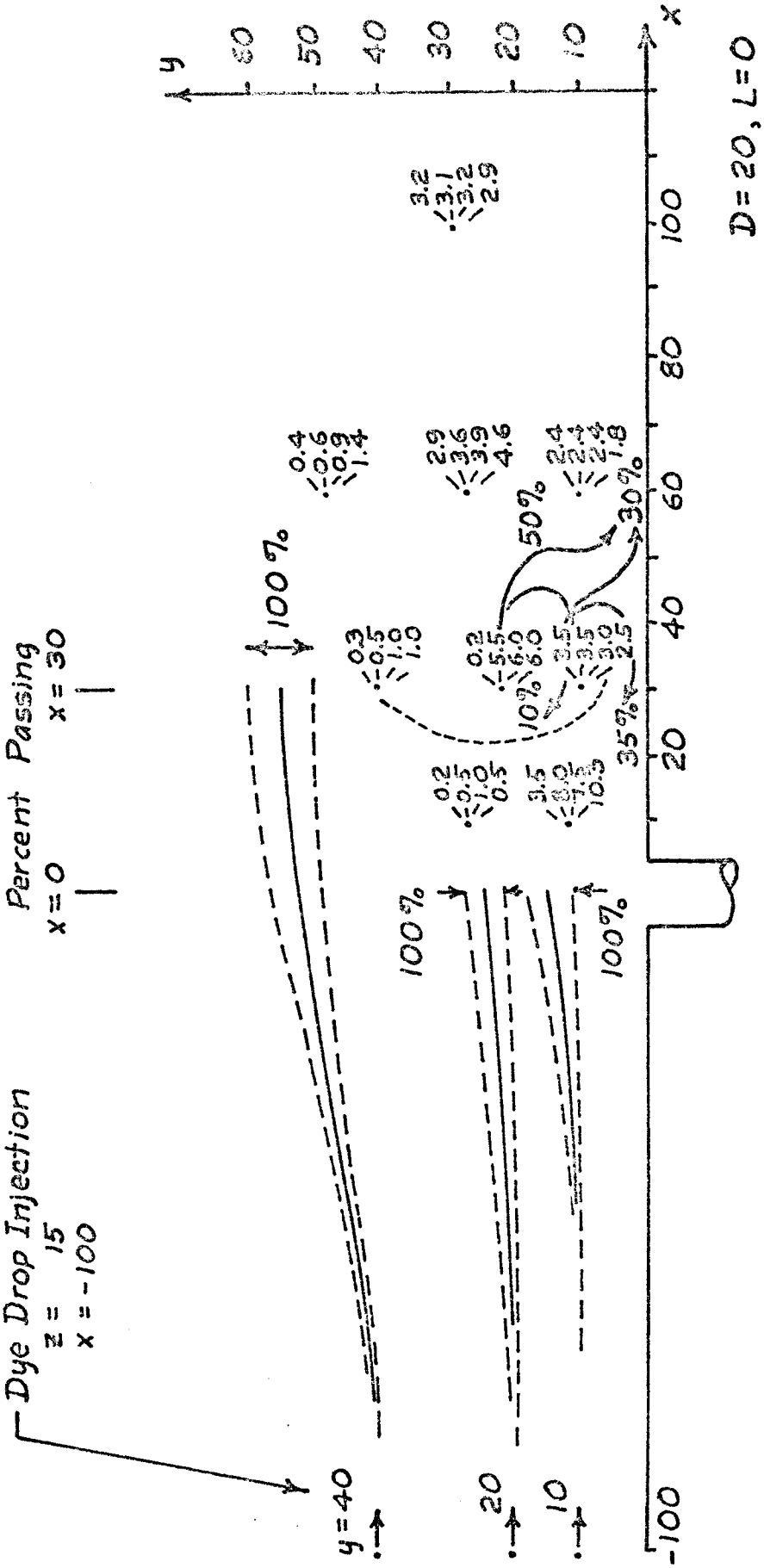

Figure 11. Fish Pathlines: D = 20 Feet, L = 0, z = 15 Feet

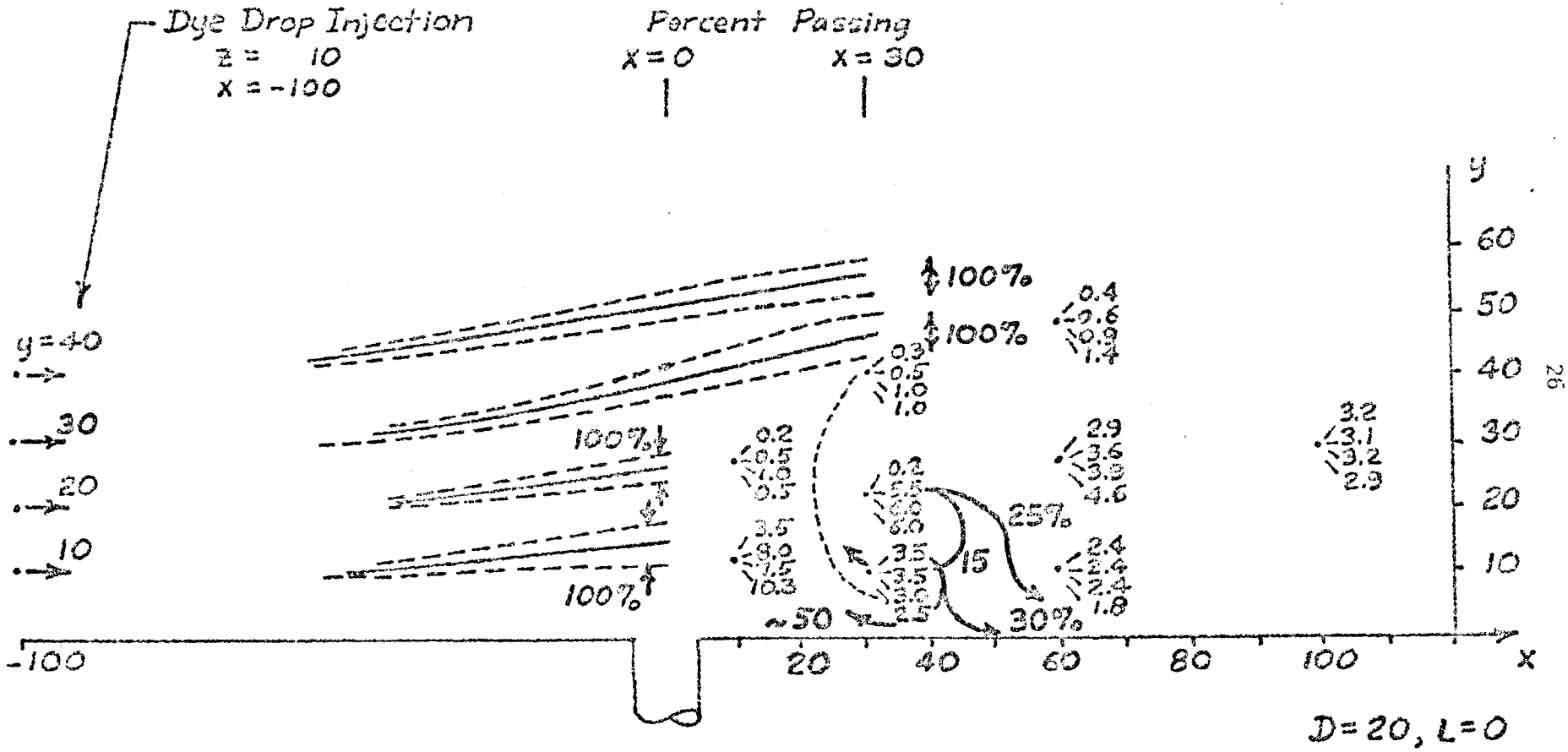

Figure 12. Fish Pathlines: D = 20 Feet, L = 0, z = 10 Feet

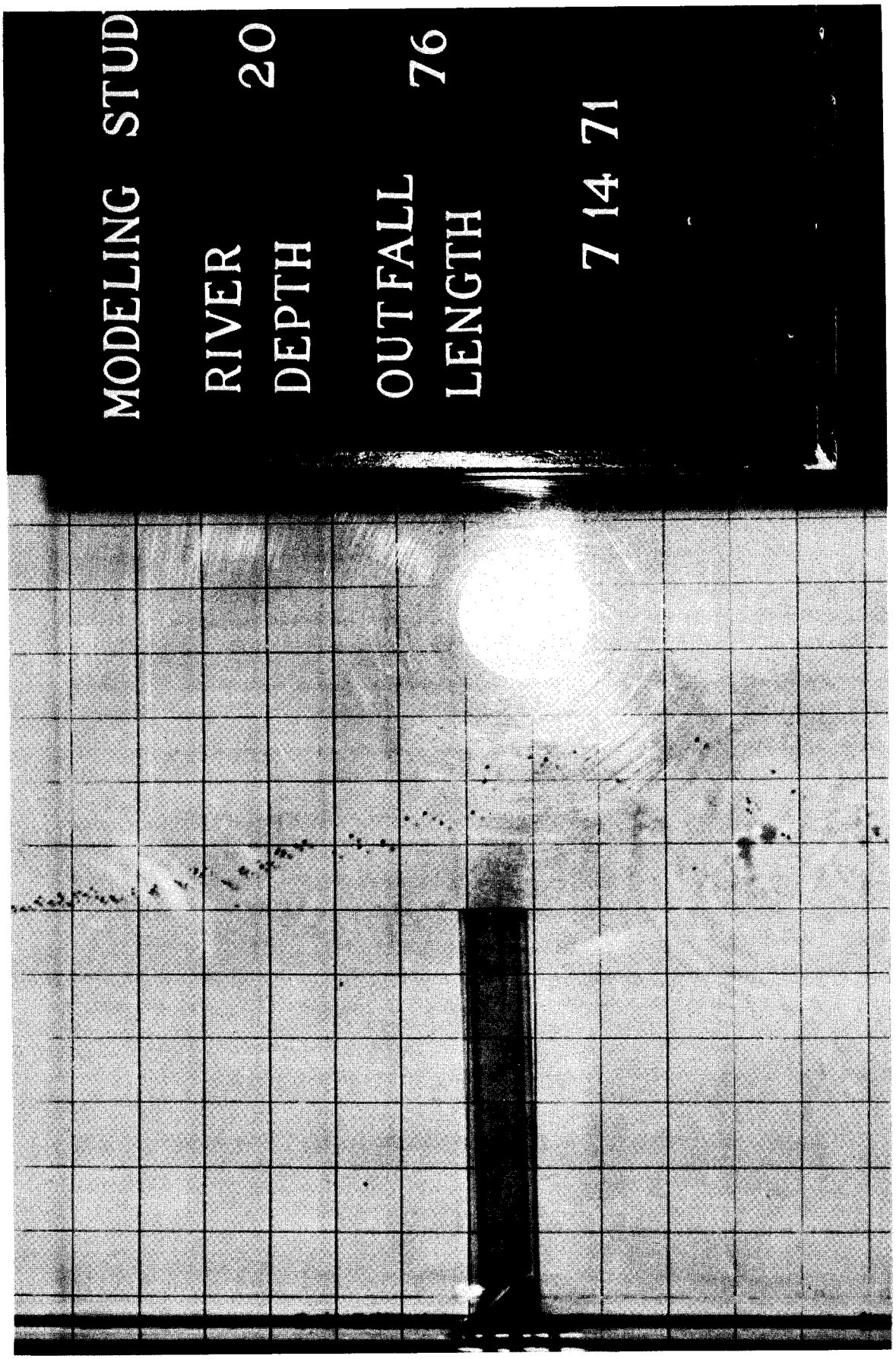

Figure 13. Photograph of Dye Drop ('Fish') Pathlines
D = 20 Feet, z = 10 Feet

rose vertically in order to pass over the conduit and/or jet, then tended to return to their original elevations. For both L = 0 and L = 76, as the bubbles moved into the diffusing jet farther downstream there was a vertical scattering of the paths as seen in elevation view.

Photograph: Figure 13 shows a representative appearance of the dye drops in the fish passage runs. Conditions for the photo run are those of Fig. 10; the bubble injection was at x = -100, y = 0, z = 10. The photograph is for illustrative rather than data purposes; there is parallax error in the x-direction. Bubble shadows are visible on the channel bottom.

The dye drops passing x = 100 are close to the inner limit of the band-width shown on Fig. 10, and at x = 40 the drops are at, or just outside of (on the rear-bank side) of the band-width limits. The drops are following a consistent path from the injection point to x = 0; for purposes of the photo, bubbles were injected much more rapidly than during the counting tests and therefore the time-space scatter is reduced. The spatial scatter of the bubbles further downstream is typical of that which takes place as the bubbles ('fish') enter the diffusing jet at and downstream from the boil.

2. D = 40 feet

Fish pathline data for the 40-foot depth are listed in Table 1 for L = 76 feet and in Table 2 for L = 0. The tabular presentation is selected because in some cases the lateral spread of bubble paths was too large to show on one plot. In cases where the bubble distribution through various 10-foot y-station gaps is not listed at the x-station which was the observation station for the particular run, the 'concentration path' column

entry indicates the band-width of the dye bubbles. Again, all dye bubbles were injected at x = -100 feet.

For the L = 76 case, dye drops moving in the upper 15 feet are not, in general, deflected outward from the near wall as much as those in the upper 10 feet for the D = 20 case; this was expected. Again, no drops ('fish') entered the initial part of the jet near the discharge portal. The fish in the upper 15 feet of water injected in-shore from the end of the outfall pass over the pipe and do not enter the jet limits upstream of x = 120 feet, the boil location. A relatively small percentage (5-10) of the bubbles injected at y = 20 and y = 0 are caught in eddies behind the boil, but as seen in Fig. 7 the ΔT to which they are exposed is less than 2°C.

Not tabulated are limited data taken for $U_0 = 0$. Although transverse scatter was comparable to that indicated in Table 1, drops released at y = 20, 0, and -20 tended to have concentration paths at essentially the same y-stations when they crossed x = 0. These bubbles were released in the top 20 feet. The net effect of the jet is to produce pathline curvatures away from the near wall.

For L = 76, bubbles released inshore of y = 0 at the injection levels given were not trapped behind the pipe as were a number in the D = 20 runs.

Paths are not deflected outward in the L = 0 case; they are also generally horizontal until the bubbles reach the boil area, where a number of drops move downward.

Table 1. Fish Pathlines: D = 40 Ft, L = 76 Ft.

Dye Release Point		Obs. Sta.	Percent of Dye Drops (Fish) Passing Between y-Stations Shown at Observation Station							Conc. Path at Obs. Station	Comments
y	z	x	← 40	20	0	-20	-40	-60 →		(y-Dist.)	
20	35	0	8	83	9					30	Jet deflects drops from near bank
	30		5	81	13	1				30	Follow inside fringe, y = -20, D.S.
	25		2	74	24						
0	35	0			26	70	4			0 > y > -10	
	30			1	39	56	4			0	
	25			4	56	40				15 > y > -15	
-20	35	0				16	75	9		-30	All drops pass over outfall pipe
	30					35	63	2		" " " " " "	
	25					43	56	1		-20	
-40	35	0					31	61	8	-45	
	30						32	67	1	-45	
	25						39	61		-45	Scatter increases with depth
20	35	110								+20 from jet centerline	90-100% pass thru boil outline; no drops caught in main jet at outlet; drops pass over jet
	30										
	25										
	20										
0	35	110			100						
	30				100						
	25				100						
	20				100						
-20	35	110								0	
	30									0	
	25									-8	

Table 2. Fish Pathlines: D = 40 Ft., L = 0

Dye Release Point		Obs. Sta.	Percent of Dye Drops (Fish) Passing Between y-Stations Shown at Observation Station										Conc. Path at Obs. Sta. (y-Dist.)	Comment
			50		40		30		20		10			
y	z	x												
40	35	0											48 ± 4	
	30												43 ± 10	Even distribution about y = 43
	25												48 ± 8	" " " " 48
20	35	0											20 ± 10	
	30												22 ± 8	
	25												24 ± 6, -12	
10	35	0											10 ± 7	
	30												10 ± 4	
	25												10 ± 8, -5	
40	35	50	33		67								48	
	30			←	75	←	→ 25	→						Most drops pass betw. y = 40, 50
	25		23		54		23							
20	35	50					12		18	→	70	→		
	30						3		32		50	15		
	25						7		53		33	7		Path curves to near bank D.S. x = 50
10	35	50									27	73	8	No drops caught in any eddies
	30										35	65		Some move back in main jet, x > 50
	25										56	44		Path curves to near wall
40	35	120		←	65	←	→ 35	→						No definite path, large band width
	30		35		30		→ 35	→						
	25		21		29		35		15					Some drops caught in down. eddy D.S. of boil
20	35	120					3		16		81			

IV. CONCLUSIONS

Jet characteristics and pathlines of simulated migrating juvenile salmon were investigated in some detail for outfall pipe lengths of L = 76 feet and L = 0, for depths D of 20 and 40 feet, for the constant ratio U_0/V = 2.45, and at the prototype temperature differential ΔT = 13°C. Visual observations of jet outlines and limited temperature data provide an adequate picture of the near-field characteristics of the cooling-water jet. Jet trajectories in the depth-constricted flow as seen in plan view were found to be sensitive neither to ΔT (and therefore the discharge densimetric Froude number) nor to geometry as characterized by various combinations of D and L for the constant d = 10 feet outfall diameter.

The 76-foot long conduit was considered long enough for determining fish pathlines past an outfall discharging at the center of a wide river channel; the zero-length outfall was considered as a limiting case.

Emphasis was placed on determining fish pathlines for the more critical 20-foot river depth. Simulated fish were injected upstream in the approach flow at depths of 5 and 10 feet beflow the surface. Pathlines are time-variant because of the turbulent channel flow, but band-widths of pathlines all originating at the same upstream release points were determined. No fish entered the hottest part of the jet, close to the discharge end of the outfall.

For the L = 76 feet, D = 20 feet tests the maximum temperature rise ΔT encountered by fish was 5°C for those caught in eddies in the boil area. Most other fish passed through the near-field of the jet at essentially river velocity, with ΔT = 3°C being an estimated maximum for

those entering the main jet and being carried to lower levels downstream from the boil. Fish approaching at 20 feet or more offshore or 30 feet or more inshore of the discharge end of the outfall experience little if any temperature rise.

There was a greater scattering effect on fish pathlines by channel flow turbulence in the 40-foot depths run, but fish approaching in the top 15 feet of water do not encounter temperature rises of more than 2°C.

V. BIBLIOGRAPHY

Ackers, P. 1969. "Modeling of Heated-Water Discharges", Chapter 6 in "Engineering Aspects of Thermal Pollution" (F. L. Parker and P. A. Krenkel, ed.), Vanderbilt University Press, pp. 177-212.

Anwar, H. O. 1969. "Behavior of Buoyant Jet in Calm Fluid", Proc. ASCE, Journal of the Hydraulics Division, 95, No. HY6, November, pp. 53-63.

Callaghan, E. E. and Ruggeri, R. S. 1948. "Investigation of the Penetration of An Air Jet Directed Perpendicularly to an Air Stream", NACA TN 1615.

Fan, L.-N. 1967. "Turbulent Buoyant Jets Into Stratified or Flowing Ambient Fluids", W. M. Keck Laboratory of Hydraulics and Water Resources Report No. KH-R-15, California Institute of Technology, Pasadena, California, 196 pp.

Fan, L.-N. and Brooks, N. H. 1966. Discussion of "Horizontal Jets in Stagnant Fluid of Other Density", Proc. ASCE, Journal of the Hydraulics Division, 92, No. HY 2, March, pp. 423-429.